Control System Design of Solid Oxide Fuel Cell and Balance of Plant in Hybrid Aircraft Propulsion System

Z. BAROT[1,*], R. CEPEDA-GOMEZ[1], D. BUZZOLA[2], and D. EWALD[3]

[1]DLR Institute of Electrified Aero Engines, Lieberoser Str. 13A, 03046 Cottbus, Germany
[2]University of Genoa, Italy
[3]Karlsruhe Institute of Technology, Germany
zalakben.barot@dlr.de, rudy.cepedagomez@dlr.de, dario.buzzola@edu.unige.it, daniel.ewald@kit.edu
Corresponding author

Keywords: solid oxide fuel cell, fuel control, utilisation supervision, temperature control, aviation.

Abstract Integrating Solid Oxide Fuel Cells (SOFCs) with Gas Turbines (GTs) offers a promising route toward high-efficiency, zero-emission aircraft propulsion. However, the strong coupling between the SOFC stack and GT introduces complex nonlinear dynamics and strict operational constraints on temperature, fuel utilization, and pressure differentials. This paper presents a multi-loop control architecture for the SOFC stack to ensure safe and efficient operation within a hybrid propulsion system. The proposed controller coordinates power, fuel utilization, and temperature regulation while maintaining limits on pressure difference and thermal gradients. Simulation studies in Simulink using an integrated SOFC model demonstrate effective power tracking, stable operation, and robust thermal management under dynamic conditions.

Introduction

The decarbonization of aviation demands novel propulsion architectures that enable both high efficiency and zero emissions. Among emerging technologies, Solid Oxide Fuel Cells (SOFCs) integrated with Gas Turbines (GTs) offer a promising solution for hydrogen-powered flight [1]. The hybrid SOFC–GT configuration combines the electrochemical efficiency of the SOFC with the high power density and flexibility of the GT, leveraging thermal and pressure synergies to enhance overall system performance [2]. However, this tight thermal and mass-flow coupling introduces complex multi-domain dynamics [3].

Rapid transients in the GT can induce pressure and flow disturbances within the SOFC manifolds, whereas the inherently slow thermal dynamics of the SOFC constrain the permissible load-change rates. Maintaining safe operation requires tight regulation of stack temperature, fuel and air utilization, and inlet–outlet pressure differences. Therefore, advanced control strategies are essential to coordinate fuel and air flows and ensure stable transient response.

Numerous studies have explored control-oriented SOFC modeling and related control strategies. Early works such as Ref. [4] developed dynamic SOFC models capturing electrochemical/thermal interactions necessary for controller design. Advanced approaches include sliding-mode control for robust nonlinear regulation [5] and model predictive control (MPC) for constraint handling via optimization [6]. For hybrid SOFC–GT systems, coordinated controllers have been developed to ensure stable load transitions and manage pressure differentials [7]. Despite these advances, limited research has addressed control architectures specifically tailored to aviation, where stringent mass, safety, and reliability requirements dominate. Recent work by Dotzauer [8] demonstrated supervisory temperature and pressure control for aircraft SOFC systems, highlighting the concept's feasibility but leaving open issues related to GT-induced disturbances and balance-of-plant integration.

The present study proposes a dedicated control architecture for the SOFC stack in hybrid SOFC–GT aircraft propulsion.

Methodology

System Overview. The proposed controller architecture comprises of three coordinated layers: a *power control loop* actuating the inlet hydrogen mass flow $\dot{m}_{\mathrm{H_2,in}}$, a *temperature control loop* actuating the inlet air mass flow $\dot{m}_{\mathrm{air,in}}$, and a *supervisory protection layer* overseeing safety constraints. The SOFC stack control system is modeled in MATLAB/Simulink, as illustrated in Fig. 1.

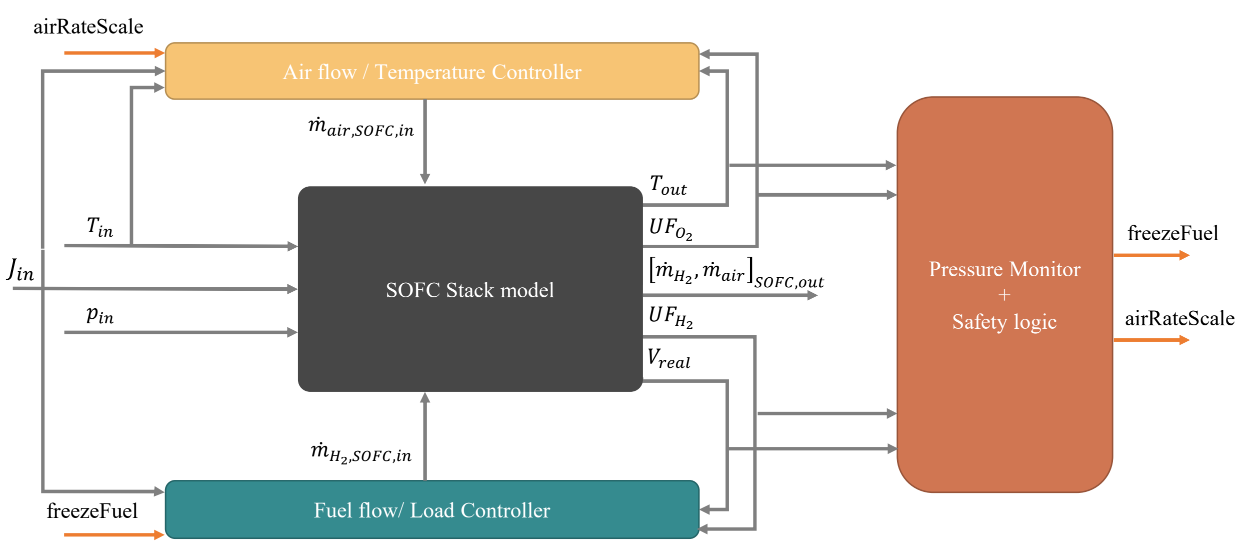

Figure 1: *Schematic of SOFC stack control architecture.*

SOFC Model Interface. For control-oriented design, the SOFC stack behavior was represented through a surrogate model developed using the Response Surface Modelling (RSM) approach. The input–output dataset for model training was generated via high-fidelity SOFC simulations. These simulations were benchmarked using operating points from a 1D steady-state SOFC model along the gas channel described in Ref. [9] and parameterized according to Ref. [10]. Based on the statistical distributions obtained from these simulations, nominal input values and corresponding variation ranges were defined. A Design of Experiments (DoE) based on a Central Composite Faced Design (CCFD) was then applied to systematically sample the operating space and generate training data. Within the RSM framework, polynomial response surfaces were constructed to approximate the mapping between inputs and outputs.

The surrogate model accurately captures the steady-state and quasi-dynamic stack response for control-oriented implementation. The RSM maps the input variables - fuel and air mass flow rates ($\dot{m}_{\mathrm{H_2,in}}$, $\dot{m}_{\mathrm{air,in}}$), inlet temperature ($T_{\mathrm{in}}$), inlet pressure ($p_{\mathrm{in}}$), and current density ($J_{\mathrm{in}}$) determined by the reference power P_{ref}, to key SOFC outputs including cell voltage (V_{real}), outlet temperature (T_{out}), outlet pressure (p_{out}), and hydrogen and oxygen utilization factors ($\mathrm{UF_{H_2}}$, $\mathrm{UF_{O_2}}$).

Fuel Flow Control Loop. The fuel flow control loop is responsible for regulating the SOFC stack power output while maintaining the desired hydrogen utilization level, thus preventing fuel starvation and ensuring efficient operation. The instantaneous electrical power generated by the stack is given by

$$P_{\mathrm{real}} = V_{\mathrm{real}} I_{\mathrm{SOFC}}. \tag{1}$$

Here, the total current (I_{SOFC}) is calculated as

$$I_{\mathrm{SOFC}} = J_{\mathrm{in}} A_{\mathrm{cell}} N_{\mathrm{cells}}, \tag{2}$$

where A_{cell} the cell area, and N_{cells} the number of cells. The combined control error (e) is then computed via

$$e = \frac{P_{\mathrm{ref}} - P_{\mathrm{real}}}{P_{\mathrm{nom}}} + \alpha \left(\mathrm{UF_{H_2,ref}} - \mathrm{UF_{H_2}} \right), \tag{3}$$

where α is weightage of utilisation factor error. The commanded hydrogen flow is

$$\dot{m}_{\mathrm{H_2}}^{\mathrm{cmd}} = \dot{m}_{\mathrm{H_2}}^{\mathrm{FF}} + u_{\mathrm{ctrl,H_2}}, \tag{4}$$

where $u_{\mathrm{ctrl,H_2}}$ is the feedback controller output and $\dot{m}_{\mathrm{H_2}}^{\mathrm{FF}}$ is a feed-forward term based on the desired utilization

$$\dot{m}_{\mathrm{H_2}}^{\mathrm{FF}} = \frac{I_{\mathrm{SOFC}} M_{\mathrm{H_2}}}{2F \, \mathrm{UF_{H_2,ref}}}. \tag{5}$$

Here, M_{H_2} is molar mass of the hydrogen, F is Faraday's constant and $\mathrm{UF}_{H_2,ref}$ is reference utilisation factor. Rate limiting and saturation mechanisms are incorporated to prevent actuator saturation and fuel starvation.

Air Flow Control Loop. The air control loop regulates stack temperature and oxygen utilization by adjusting the cathode airflow. Its primary goal is to maintain the operating temperature within a prescribed safety band, ensuring thermal balance between the anode and cathode while preventing oxygen starvation. The feed-forward airflow is derived from Faraday's law as

$$\dot{m}_{\mathrm{air}}^{\mathrm{FF}} = \gamma_{\mathrm{ff}} \frac{I_{\mathrm{SOFC}} M_{\mathrm{air}}}{4F \, x_{\mathrm{O_2}} \, \mathrm{UF_{O_2,ref}}}, \tag{6}$$

where M_{air} is the molar mass of air, $x_{\mathrm{O_2}}$ is the oxygen molar fraction in air, and γ_{ff} is a tuning coefficient accounting for excess air. Similar to the fuel control loop, the commanded air flow is defined as

$$\dot{m}_{\text{air}}^{\text{cmd}} = \dot{m}_{\text{air}}^{\text{FF}} + u_{\text{ctrl,air}}, \tag{7}$$

where $u_{ctrl,air}$ is the control action modulated by the temperature feedback compensator based on the deviation from the temperature operating band $[T_{\min} + b,\, T_{\max} - b]$, where b is buffer region. Safety guards apply corrective boosts to the air command when outlet pressure or oxygen utilization approach unsafe limits:

$$\dot{m}_{\text{air}}^{\text{cmd}} = \dot{m}_{\text{air}}^{\text{cmd}} + k_p \max(0,\, p_{\min} - p_{\text{out}}) + k_u \max(0,\, UF_{O_2,\min} - UF_{\text{O}_2}), \tag{8}$$

where k_p and k_u are gain coefficients enforcing corrective airflow boosts. Finally, a temperature rate governor constrains the air command to maintain the rate of temperature change within prescribed bounds. In case of violation where temperature rate exceeds $\dot{T}_{\max}$, the air command is updated as:

$$|\dot{T}_{\text{out}}| > \dot{T}_{\max} \quad \Rightarrow \quad \dot{m}_{\text{air,cmd}} \leftarrow \dot{m}_{\text{air,prev}} + \lambda\, \text{sign}(-\dot{T}_{\text{out}})\, \Delta t \tag{9}$$

where $\lambda < 1$ scales the corrective adjustment. This constraint mitigates rapid heating or cooling, preventing thermal stress and protecting the stack's structural integrity.

Supervisory Protection Layer. The supervisory layer monitors the differential pressure $p_{\text{loss}} = p_{\text{in}} - p_{\text{out}}$ and its derivative based on sampling time t_S. When pressure deviations exceed safe limits, two corrective actions are activated: (i) freezeFuel, which temporarily holds the fuel command to avoid further divergence, and (ii) airRateScale, which adaptively scales the the cathode airflow to attenuate pressure transients. These measures ensure smooth flow dynamics and prevent mechanical stress on the stack. Start-up interlocks further restrict fuel supply when temperature or utilization fall outside admissible ranges.

Results and Discussion

The closed-loop responses of the integrated SOFC control structure, for a fixed power demand set point (P_{ref}), is presented in Fig. 2. Since no load transients were applied at this stage, the results primarily reflect the controller steady-state regulation capability and its initial transient convergence from startup. The fuel controller (see Fig. 2a) drives the stack current density J_{in} and cell voltage V_{real} toward their respective reference conditions. A short initial overshoot appears as the state converges, after which the electrical variables settle close to the reference values ($V_{\text{ref}} \approx 0.6$ V) with negligible steady-state error. The commanded hydrogen and air flows (see Fig. 2b), $\dot{m}_{\text{H}_2\text{,in}}$ and $\dot{m}_{\text{air,in}}$, exhibit first-order transients before stabilizing within their $\pm 2\%$ tolerance bands around the nominal set points ($\dot{m}_{\text{H}_2\text{,ref}} = 0.02995$ kg/s, $\dot{m}_{\text{air,ref}} = 2.166$ kg/s). These transients reflect the initialization of the feed-forward and rate-limited dynamics in both the fuel and air controllers. Overall, these preliminary results confirm that the hierarchical control structure achieves stable convergence to the nominal steady state without inducing excessive overshoot or cross-coupling.

The air-side loop regulates outlet pressure p_{out} and temperature T_{out} to their operating targets ($p_{\text{ref}} \approx 9.9$ bar, $T_{\text{out,ref}} \approx 815$ °C). The temperature shows a gradual rise due to its larger thermal time constant, while the pressure transient is well damped and quickly returns to nominal after the initial air-flow adjustment (see Fig. 2c). No oscillations or instabilities are observed, indicating adequate tuning of the asymmetric air flow gains and the temperature slew limiter. The supervisory layer responds effectively to simulated pressure-loss events by temporarily freezing the fuel command and scaling air rate limits. This action

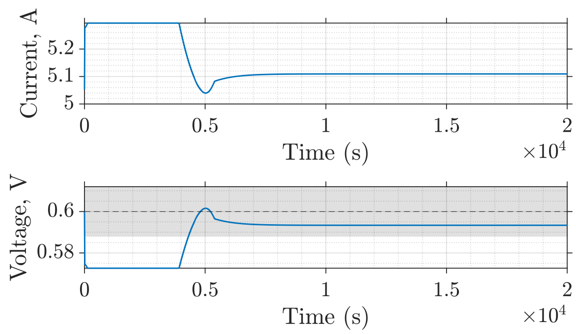

(a) *Voltage and current response.*

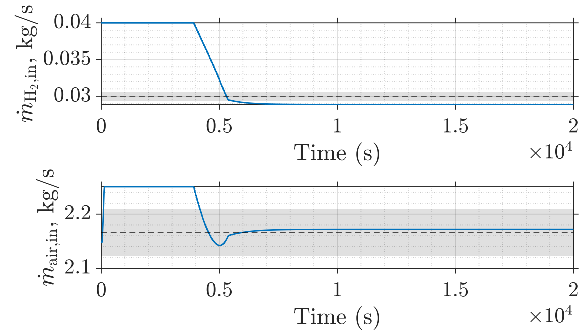

(b) *Hydrogen and air mass flow rates.*

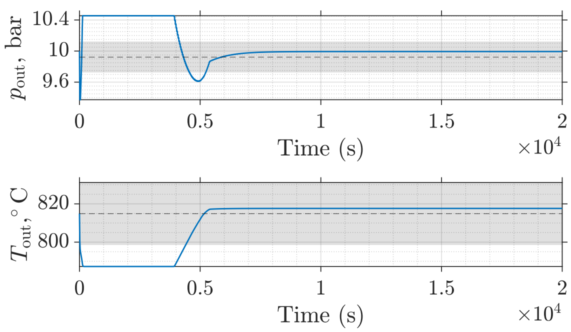

(c) *Outlet pressure and temperature.*

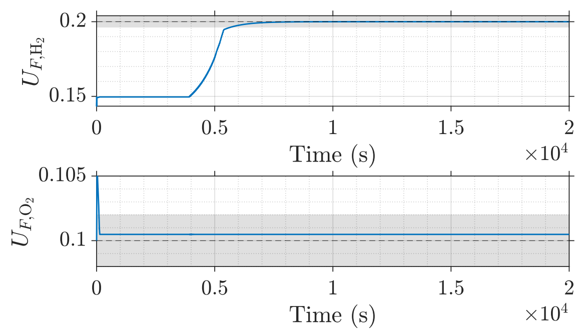

(d) *Fuel and oxygen utilization factors.*

Figure 2: *SOFC stack control responses with reference values*

reduces p_{loss} below the warning threshold without inducing large thermal transients. Both utilizations, $UF_{\mathrm{H_2}}$ and $UF_{\mathrm{O_2}}$, converge smoothly to their nominal references (0.20 and 0.10, respectively), remaining well within the defined soft limits (see fig. 2d).

Conclusion and Future Work

A hierarchical SOFC control architecture for hybrid SOFC–GT aircraft configuration is proposed. The main contributions include: (i) a fuel-flow control law jointly regulating power and hydrogen utilization, (ii) a pressure-aware air control strategy for temperature-band regulation, and (iii) a supervisory protection layer managing pressure losses and start-up interlocks. The control design is validated via simulations based on a polynomial response surface SOFC model.

The proposed control strategy achieved stable power tracking, effective thermal regulation, and compliance with key safety constraints under dynamic conditions. Minor startup transients are observed at initialization. To study these further, full load-change studies must be conducted in subsequent dynamic validation tests.

Future work will extend this study by: (i) conducting parameter envelope sweeps and robustness analyses, (ii) detailed discussion and explanation of control laws, (iii) incorporating actuator and manifold dynamics, (iv) integrating the SOFC model with a gas turbine for hybrid propulsion simulations, and (v) enhancing controller design to include balance-of-plant (BoP) components such as inlet heat exchangers.

Acknowledgement

This project has received funding from the European Union's Horizon Europe research and innovation programme under grant agreement No. 101138488 and by the UK Research and Innovation (UKRI) funding guarantee under the project reference 10106893. Views and opinions expressed are however those of the author(s) only and do not necessarily reflect those of the European Union, UKRI or CINEA. Neither the European Union nor the granting authorities can be held responsible for them.

References

[1] L. Eichhorn, J.-C. Jeske, S. Kazula, D. Dimos, S. de Graaf, D. Ewald, A. Weber, L. Mantelli, and M. L. Ferrari. Review and evaluation of solid oxide fuel cell-gas turbine hybrid system design choices for aviation. In *Proceedings of the 16th European SOFC & SOE Forum (EFCF)*, Lucerne, Switzerland, July 2024. July 2–5, 2024.

[2] D. San Benito Pastor, E. Pontika, S. de Graaf, D. Ewald, A. Weber, S. Kazula, M. L. Ferrari, and P. Laskaridis. Hydrogen-powered integrated power and propulsion system (ipps) architecture for sustainable aviation: leveraging synergies between gas turbine and solid oxide fuel cells. In *TSAS 2025 Conference Proceedings*, Toulouse, France, January 2025. January 28–30, 2025.

[3] L. Mantelli, A. Dubey, D. Buzzola, M. L. Ferrari, E. Pontika, S. Kazula, D. Ewald, A. Weber, and S. de Graaf. Methodology for exploring sofc system layouts in a highly integrated hybrid propulsion system. In *Turbo Expo: Power for Land, Sea, and Air 2025*, Memphis, Tennessee, USA, July 2025. July 16–20, 2025.

[4] N. Lu, Q. Li, X. Sun, and M. A. Khaleel. Dynamic modeling in solid-oxide fuel cells controller design. In *IEEE Conference Proceedings*, 2007. IEEE Publication.

[5] L. Zhang, S. Shi, and X. Li. A high efficiency and fast load oriented sliding mode controller for solid oxide fuel cell system. In *Proceedings of the World Congress on Intelligent Control and Automation (WCICA)*, 2018.

[6] Y. Li, J. Shen, and J. Lu. Constrained model predictive control of a solid oxide fuel cell based on genetic optimisation. *Journal of Power Sources*, 196:5873–5880, 2011.

[7] X. Wang, X. Lv, X. Mi, C. Spataru, and Y. Weng. Coordinated control approach for load-following operation of sofc–gt hybrid system. *Energy*, 248:123548, 2022.

[8] N. A. Dotzauer. Control scheme of a solid oxide fuel cell system for regional aircraft. In *AIAA Scitech Forum*, 2025.

[9] D. Klotz, J.P. Schmidt, A. Weber, and E. Ivers-Tiffée. Performance model for large area solid oxide fuel cells. *Journal of Power Sources*, 259:65–75, 2014.

[10] A. Leonide, Y. Apel, and E. Ivers-Tiffée. Sofc modeling and parameter identification by means of impedance spectroscopy. *ECS Transactions*, 19(20):81, 2009.